MAX-DOAS measurements of urban air pollution from an elevated mountain site: Technical setup and experience from the first two years of observations.

Jochen Stutz[1,2] , Ross Cheung[1,2], Stanley P. Sander[2,3], D. Chen[2], and Q. Li[1,2]

[1]Department of Atmospheric and Oceanic Sciences, UCLA
[2]Joint Institute for Regional Earth System Science and Engineering, UCLA
[3]NASA Jet Propulsion Laboratory, Caltech

Motivation

- Longterm observation of spatial and temporal distribution of trace gases in an the Los Angeles airshed, to:
  - Monitor levels of pollutants (NO_2, HCHO, SO_2, aerosol)
  - Improve air quality and regional models
  - Validate and improve emission inventories, in particular for NO_X and GHG

<u>South Coast Air Basin</u>
25,824 km^2
16.8 million people

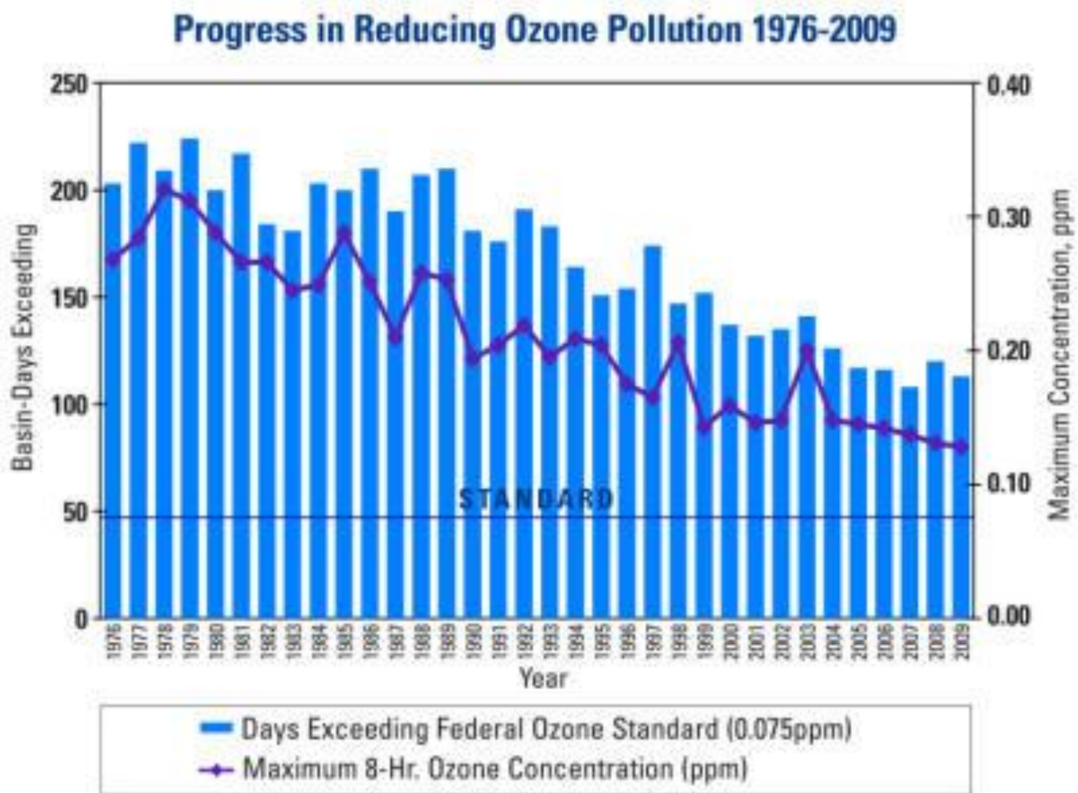

- Owned by NASA's Jet Propulsion Laboratory
- Mt. Wilson, CA, with a near full view of the LA basin
  - Latitude: 34° 13' 28'' N
  - Longitude: 118° 3' 25'' W
- Altitude: 1706 meters ASL

  Mostly above the boundary layer

Instruments:

- UCLA Multi-Axis Differential Optical Absorption Spectrometer
- JPL Near-IR Fourier Transform Spectrometer
- *Meteorological measurements*
- *Various in-situ instruments*

Measurements started in mid-May 2010 and are continuing

Viewing Geometries

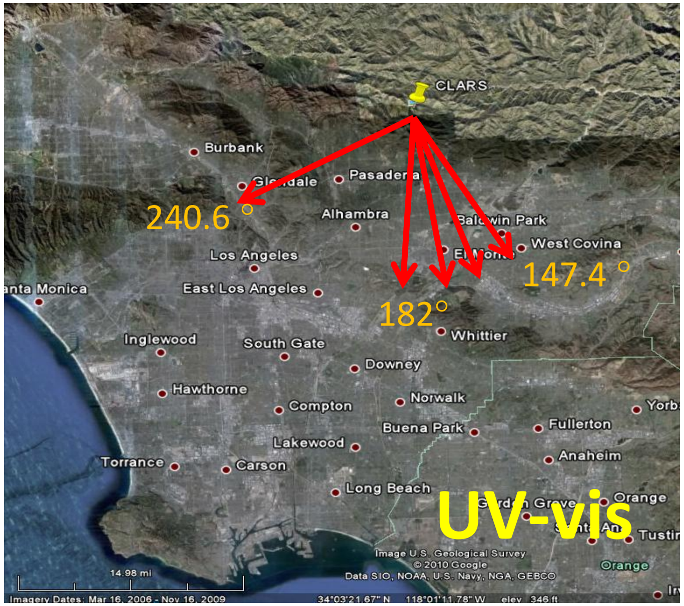

UV-vis Azimuth Angles	147.4°, 160°, 172.5°, 182°, 240.6°
UV-vis Elevation Angles	-10°, -8°, -6°, -4°, -2°, 0°, 3°, 6°, 90°

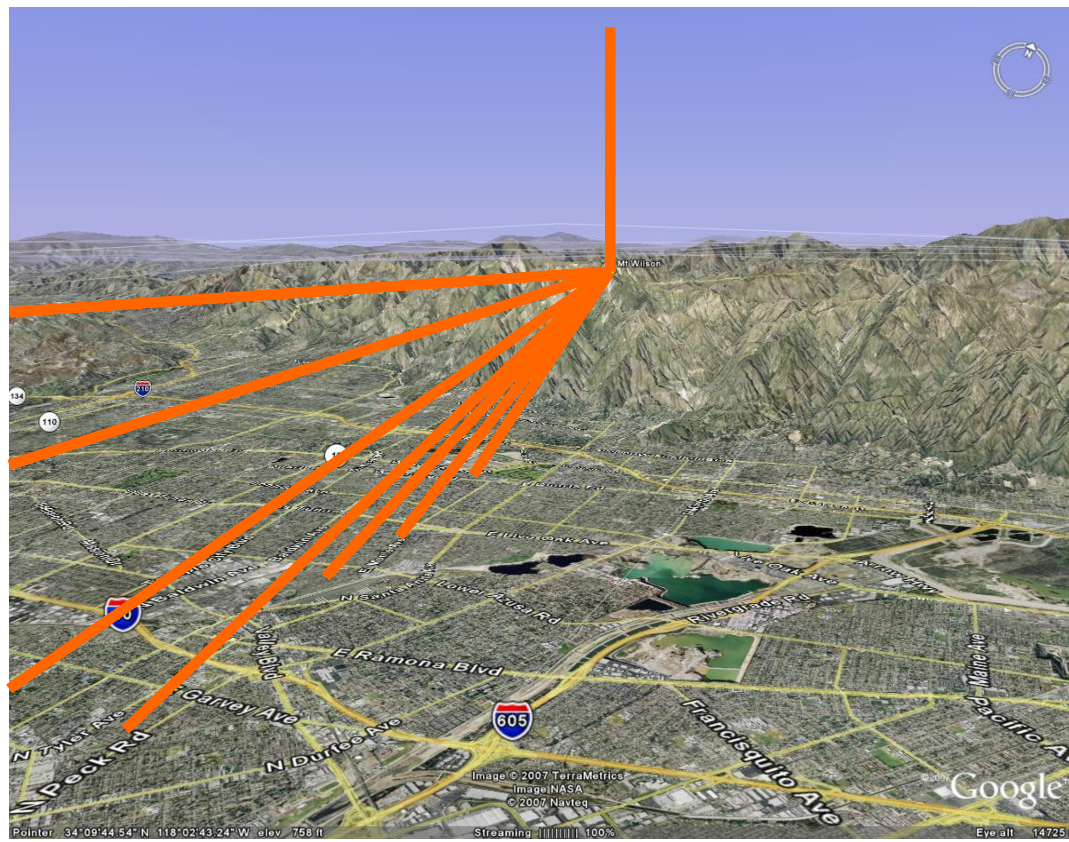

The Mt. Wilson MAX-DOAS

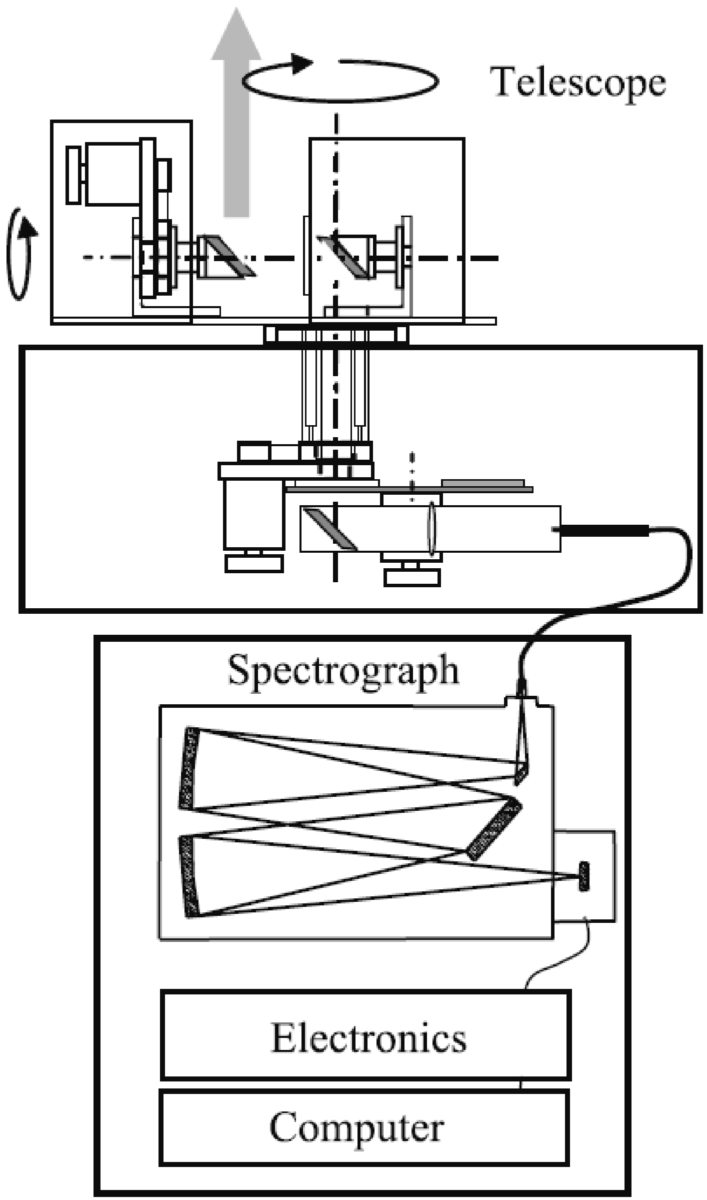

- 2π scanner / Field of view: 0.4°
- Acquisition time: 45 seconds
- DOASIS for aquis. + retrieval

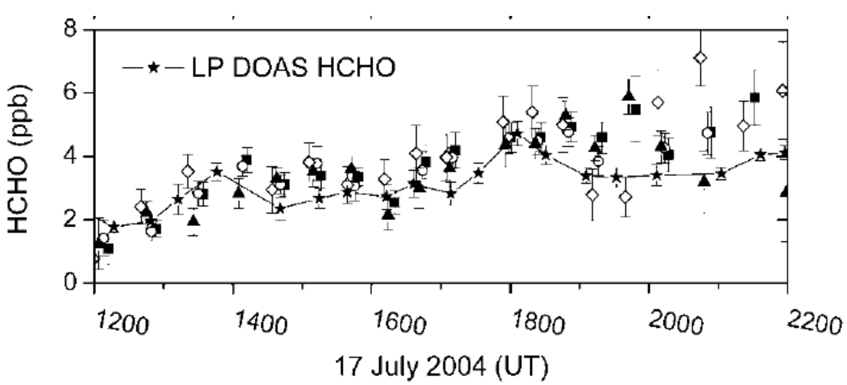

Pikelnaya et al., 2007

Spectrometer

- 300mm Czerny Turner Spectrometer, 600 g/mm grating
  Optimized for low straylight by addressing
  - re-entrant light
  - UV bandpass filter (Schott UG5)

  $\rightarrow$ Straylight (with Xe-arc Lamp) between 300-420nm $< 0.16\%$
  (not counting reflection on detector window)

- Thermally stabilized to ± 0.1 K
  (~0.1 pixel per K drift)

- Spectral Resolution: 0.7nm

- Two wavelength ranges
  UV (335-465 nm)
  visible (465-595 nm)

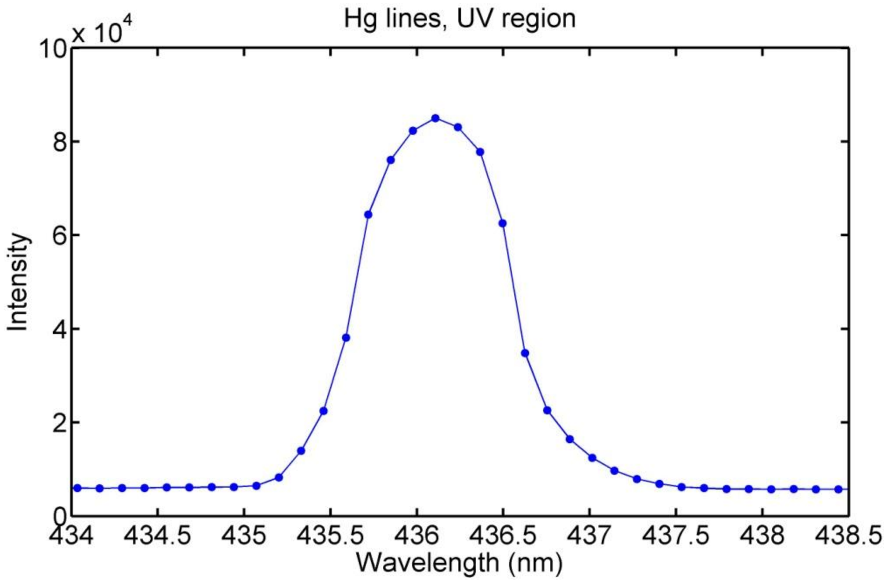

Detector

Hamamatsu Photodiode Array
1024 pixel

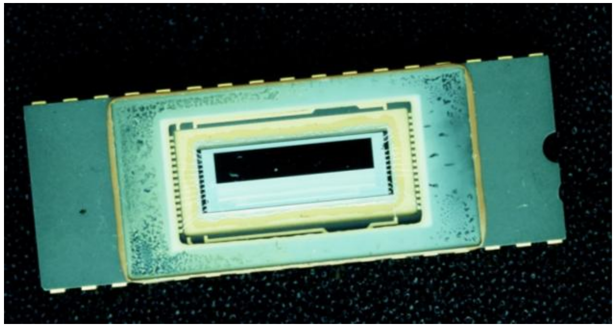

- Cooled to -20±0.1° C
- Linearity better than 0.3%

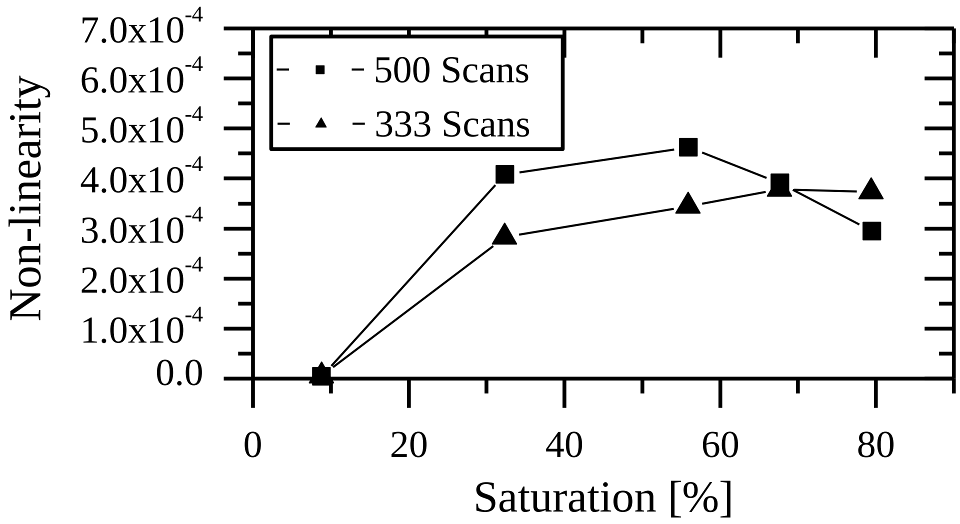

From Previous PDA Version

- Auto-exposure to maintain saturation level (commonly used now!)
- Higher readout-noise compared to CCD, but higher capacity

Data Analysis

Combined linear non-linear least squares fitting (Platt and Stutz, 2008) with temporally close Zenith reference, Ring and various trace gas absorptions

Species	Scan	Wavelength Interval (nm)	Fitted Spectral References	Detection Limit
O_4	UV	350-390	NO_2, O_4, HCHO, HONO	$7*10^{41}$ molec^2/cm^5
O_4	Vis	464-506.9	NO_2, glyoxal, O_4, H_2O	$8*10^{41}$ molec^2/cm^5
O_4	Vis	519.8 - 587.7	NO_2, O_4, O_3, H_2O	$5*10^{41}$ molec^2/cm^5
HCHO	UV	323.4-350	HCHO, O_4, O_3, HONO	$5*10^{15}$ molec/cm^2
NO_2	UV	323.4-350	HCHO, O_4, O_3, HONO	$3*10^{15}$ molec/cm^2
NO_2	UV	419.5-427.9 & 432.4-447	NO_2, glyoxal, O_4, H_2O	$1*10^{15}$ molec/cm^2
NO_2	Vis	464-506.9	NO_2, glyoxal, O_4, H_2O	$1*10^{15}$ molec/cm^2
NO_2	Vis	519.8 - 587.7	NO_2, O_4, O_3, H_2O	$2*10^{15}$ molec/cm^2
After 1/2011				
NO_2	UV	332.8-377.8	HCHO, O_4, O_3, HONO	$2*10^{15}$ molec/cm^2
NO_2	UV	416.3-456.6	NO_2, glyoxal, O_4, H_2O	$1*10^{15}$ molec/cm^2
HCHO	UV	332.8-377.8	HCHO, O_4, O_3, HONO	$2*10^{16}$ molec/cm^2

O_4: Hermans et al, 1999, O_3: Voigt et al. 2001, NO_2: Voigt et al., 2002 H_2O: HITRAN, glyoxal: Volkamer et al. 2005, HCHO: Cantrell et al. 1990, HONO: Stutz et al., 2000

Viewing geometry

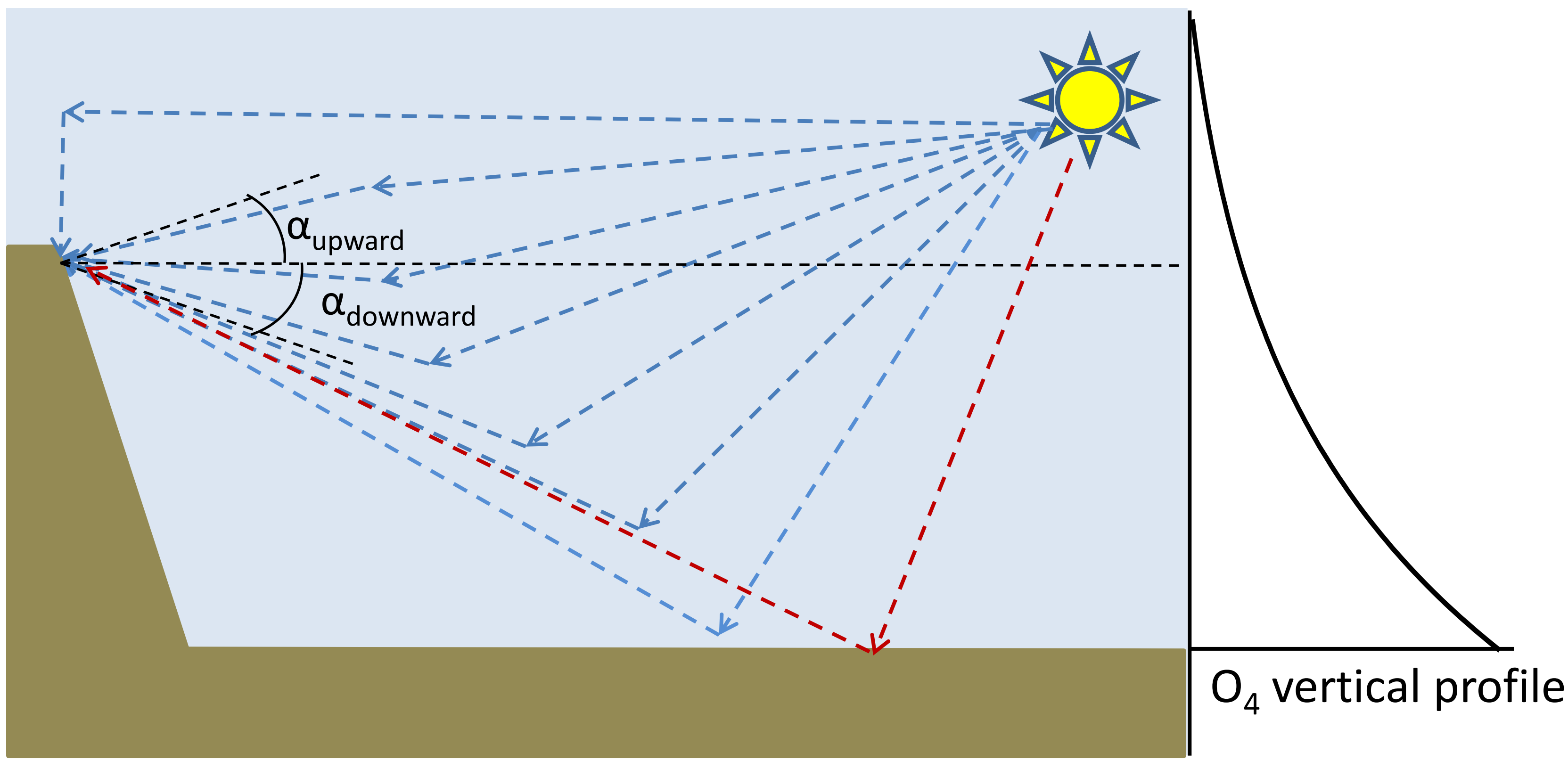

- Slant Column Density (SCD) : $$SCD = \int_0^L c(s) \cdot ds$$
- **UV-vis** Differential slant column densities (DSCD) obtained by removing temporally close zenith zenith $$DSCD = SCD_{off-axis} - SCD_{zenith}$$

UV-vis Radiative Transfer

Example of Differential Box Air Mass Factors for MAX-DOAS in the UV

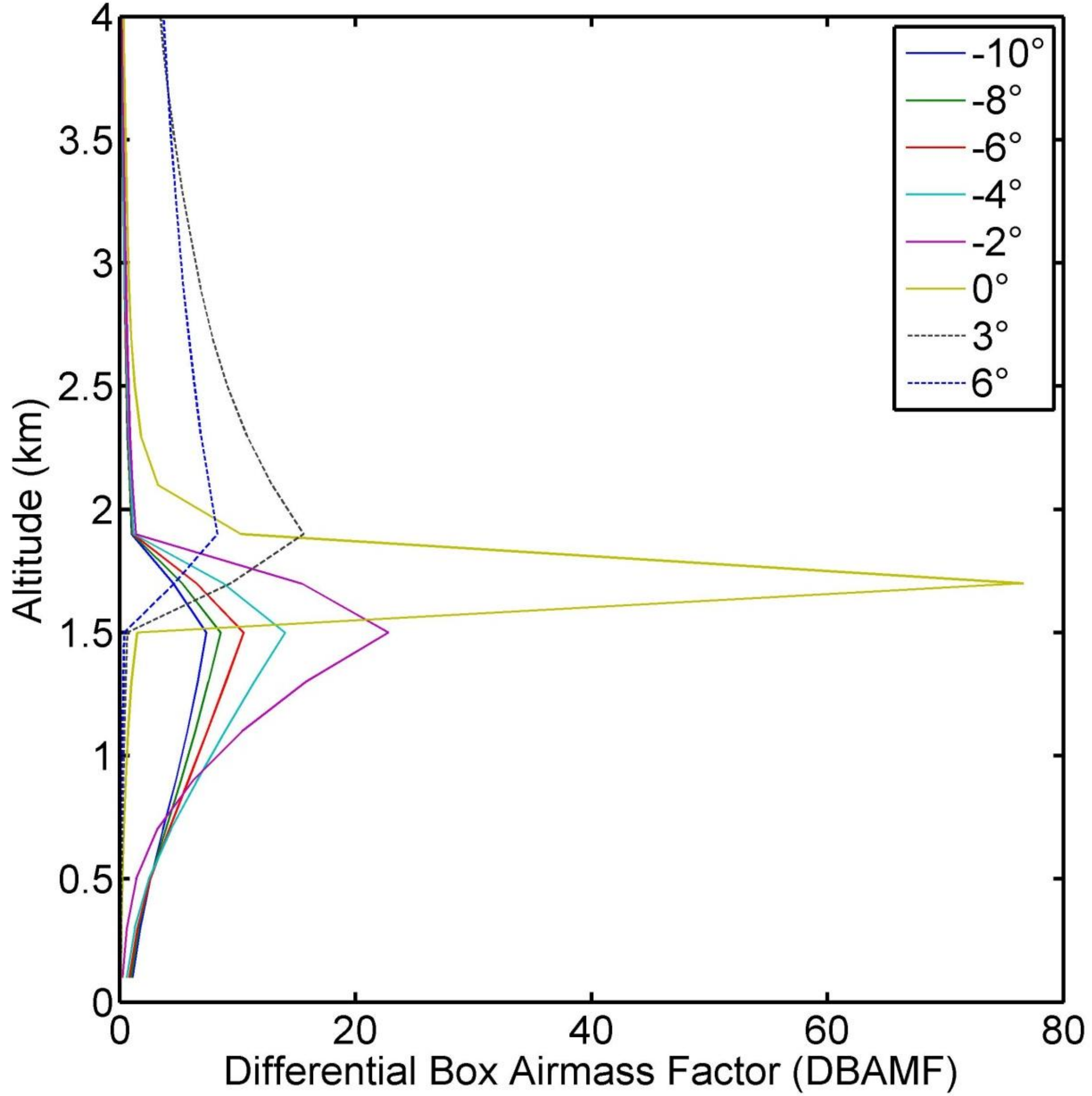

Wavelength Dependence of UV-Vis DSCD

All figures are in the same viewing direction

DSCD: (5.3 ± 0.3) x 10^{16}

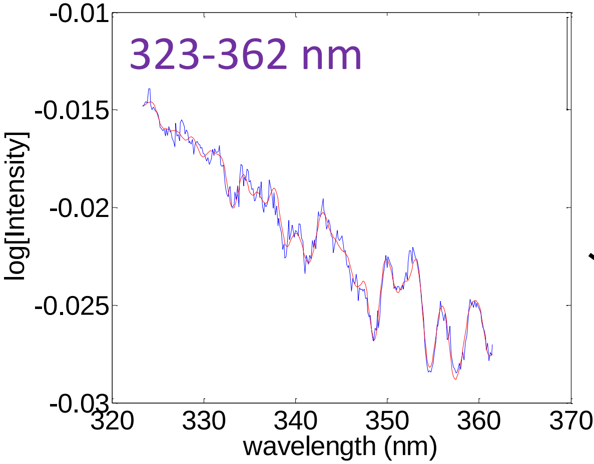

DSCD: (7.4 ± 0.2) x 10^{16}

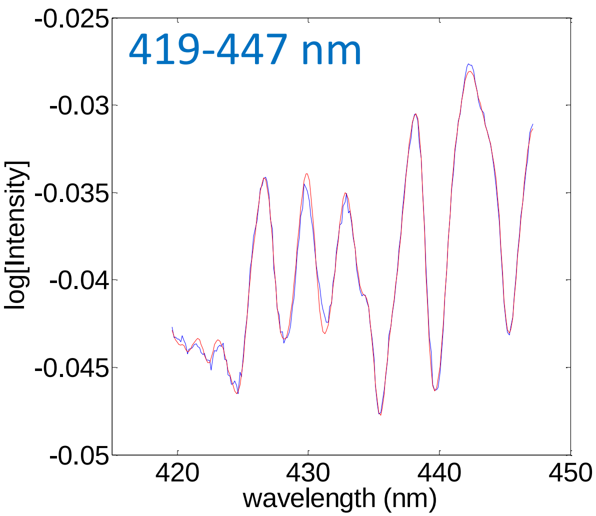

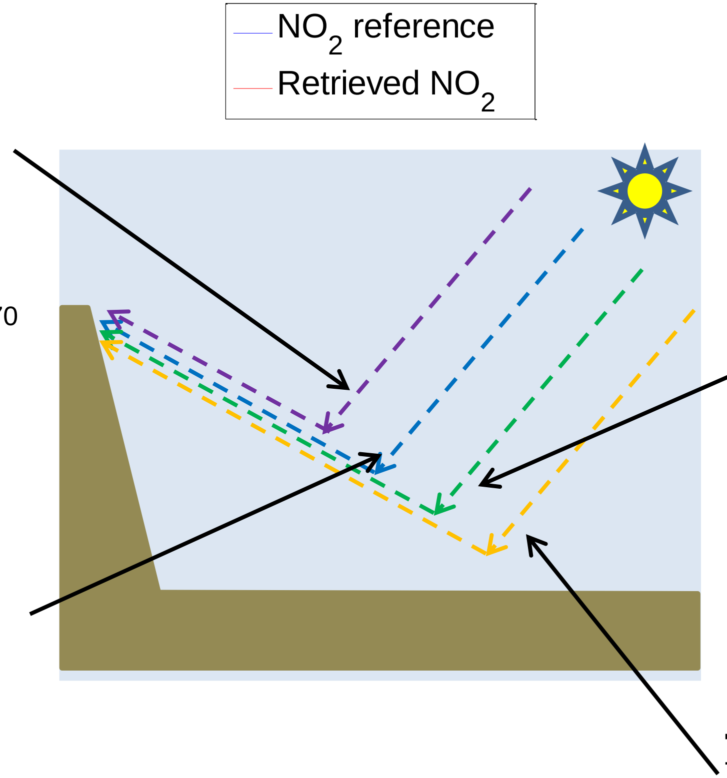

DSCD: (7.3 ±0.1) x 10^{16}

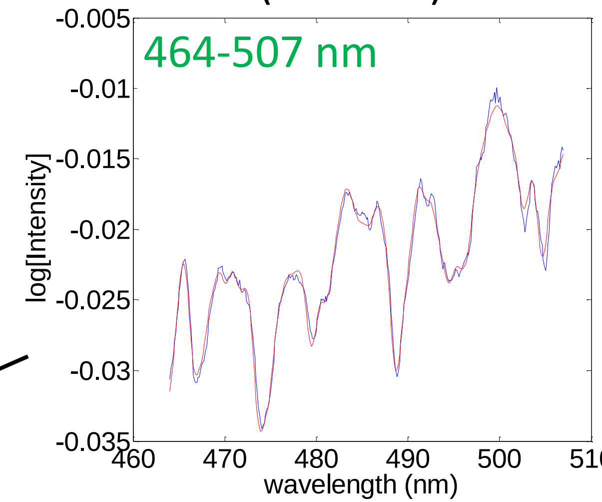

DSCD: (10 ± 0.2) x 10^{16}

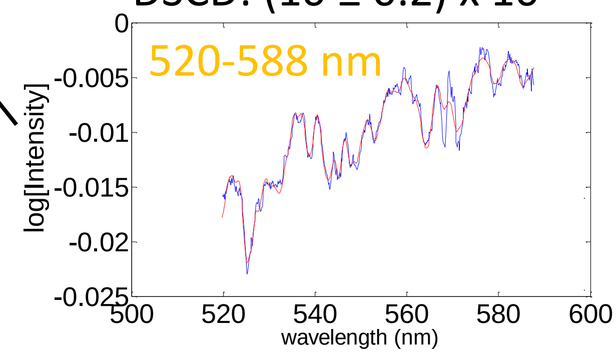

Path length is wavelength dependent due to scattering effects

Example of DSCD Wavelength dependence

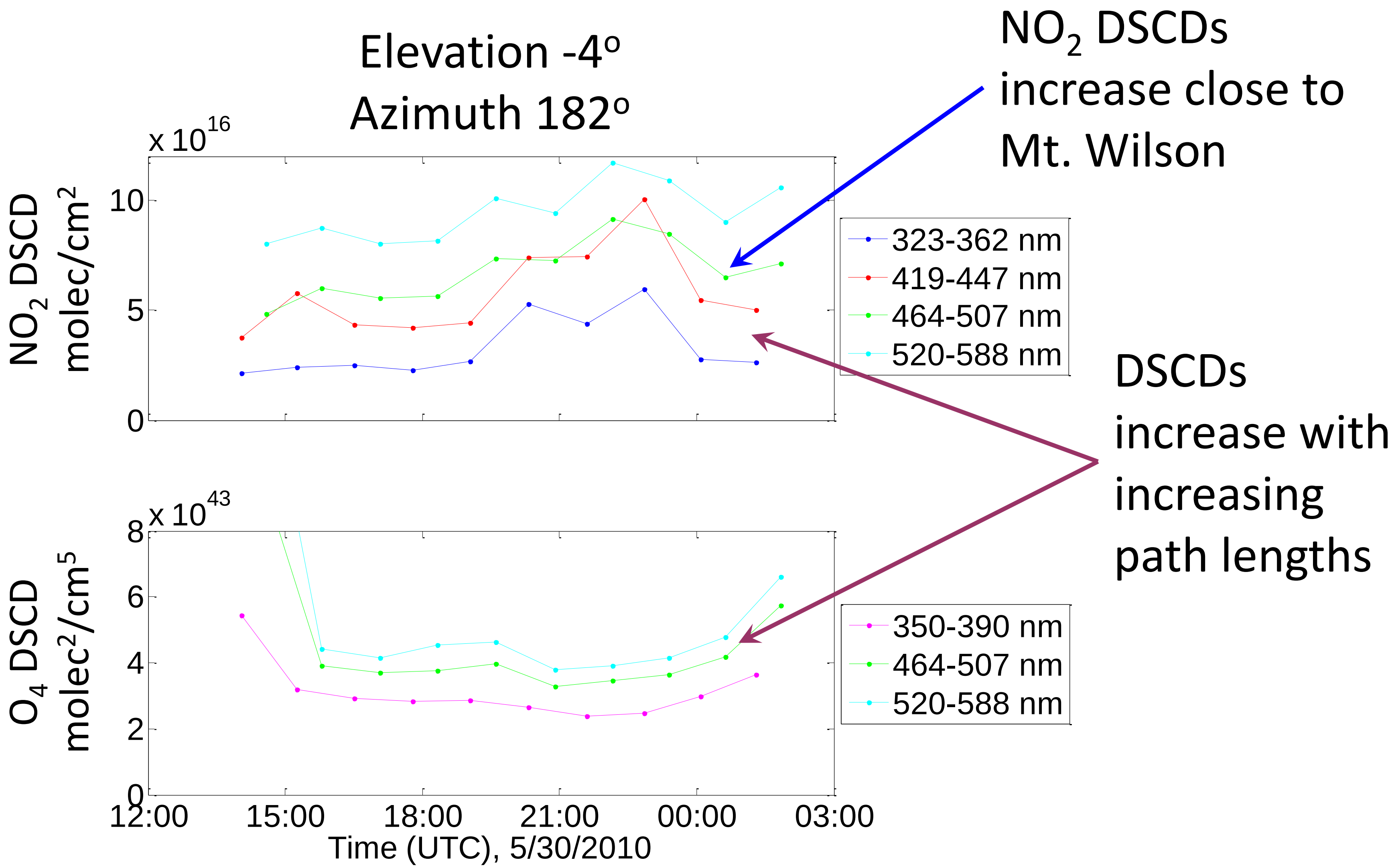

Obtaining NO_2 and O_4 DSCDs at different wavelengths adds valuable information on spatial extent and radiative transfer

Overview of MAX-DOAS data on May 31, 2010

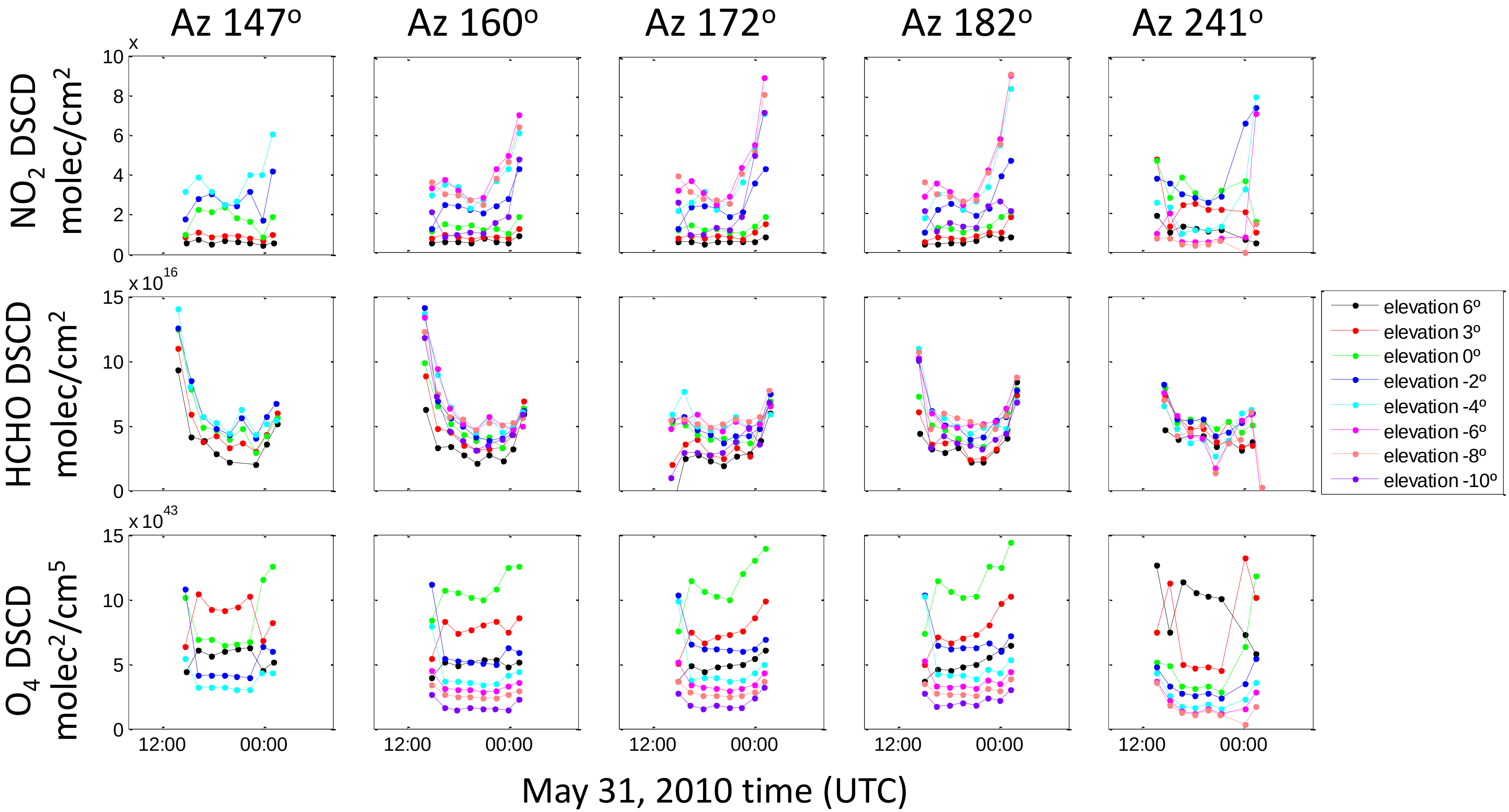

Cloud Filtering

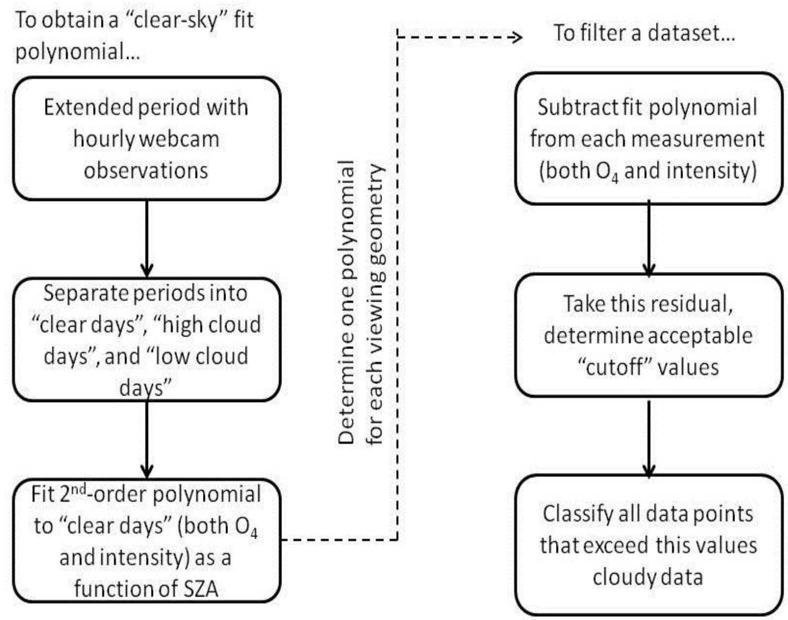

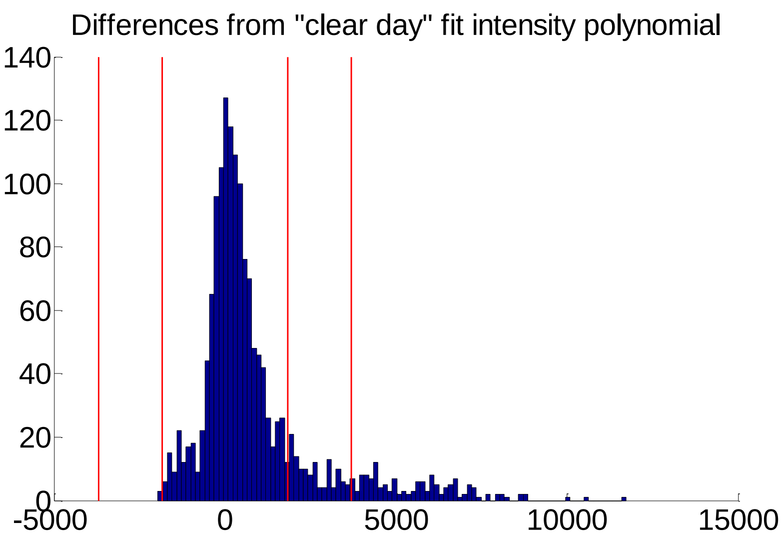

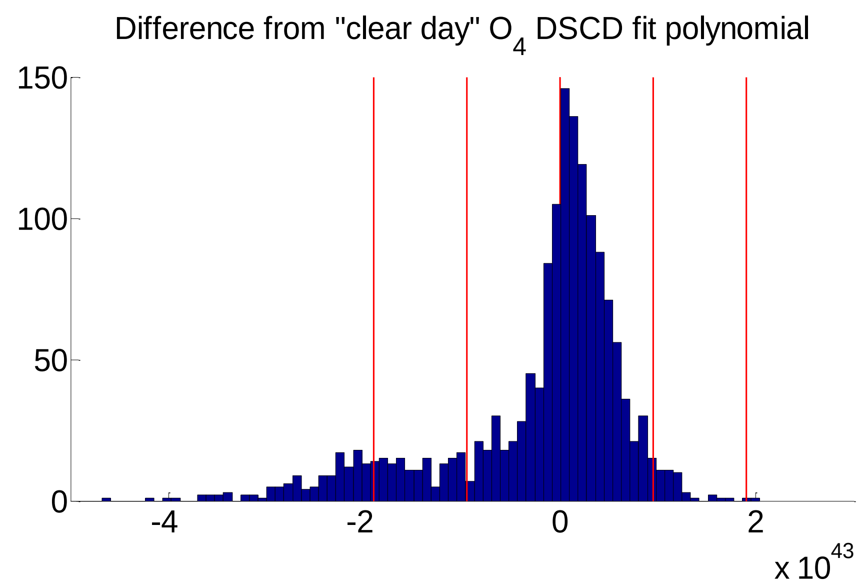

Application: Comparison with WRF-Chem

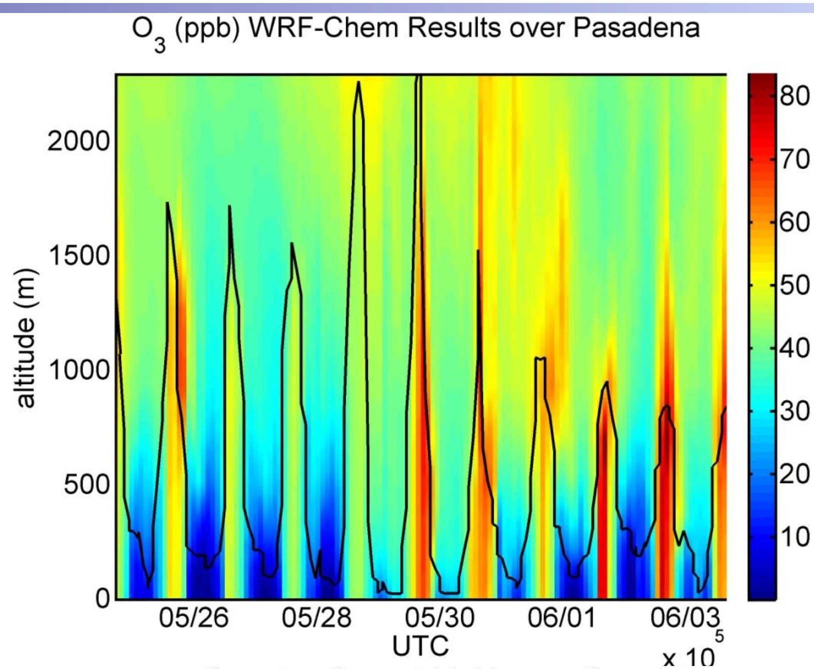

WRF-Chem model:

- 4x4km resolution,
- assimilated Meteorology
- Chemistry CBMZ
- Aerosol: MOSAIC(4 bin)
- Adjusted 2005 ARB EI
- Validated for CalNex

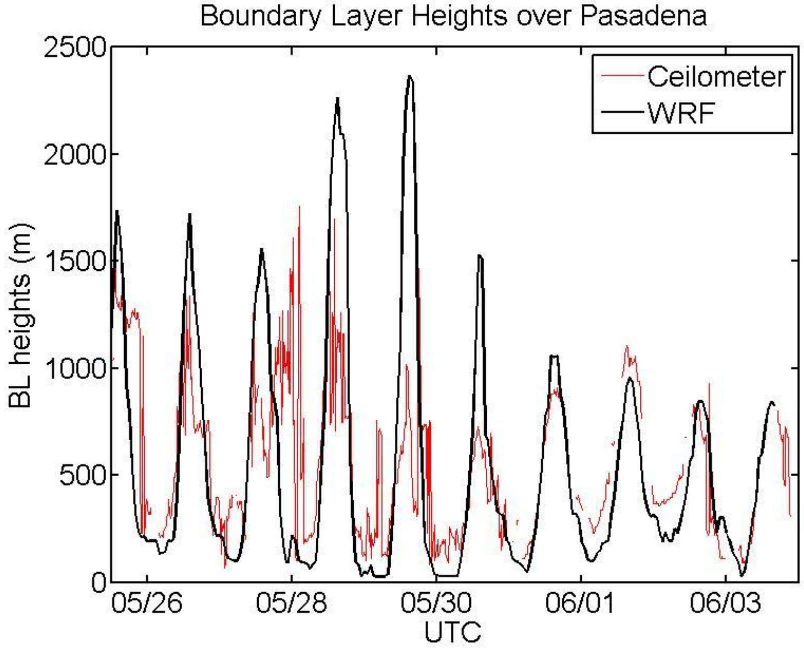

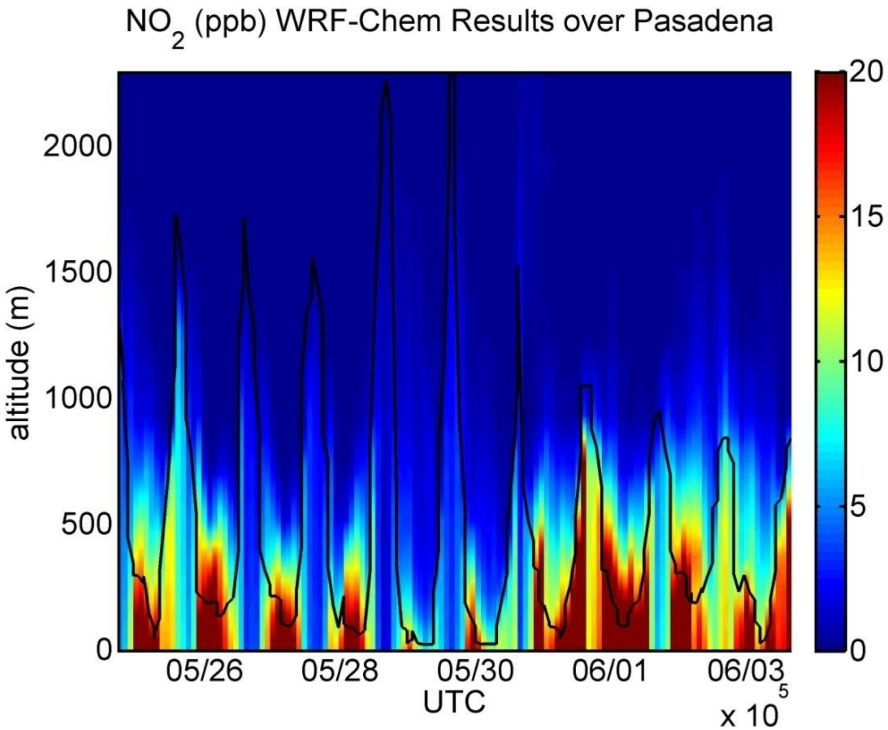

Modeled Vis Aerosol Extinction (km^{-1})

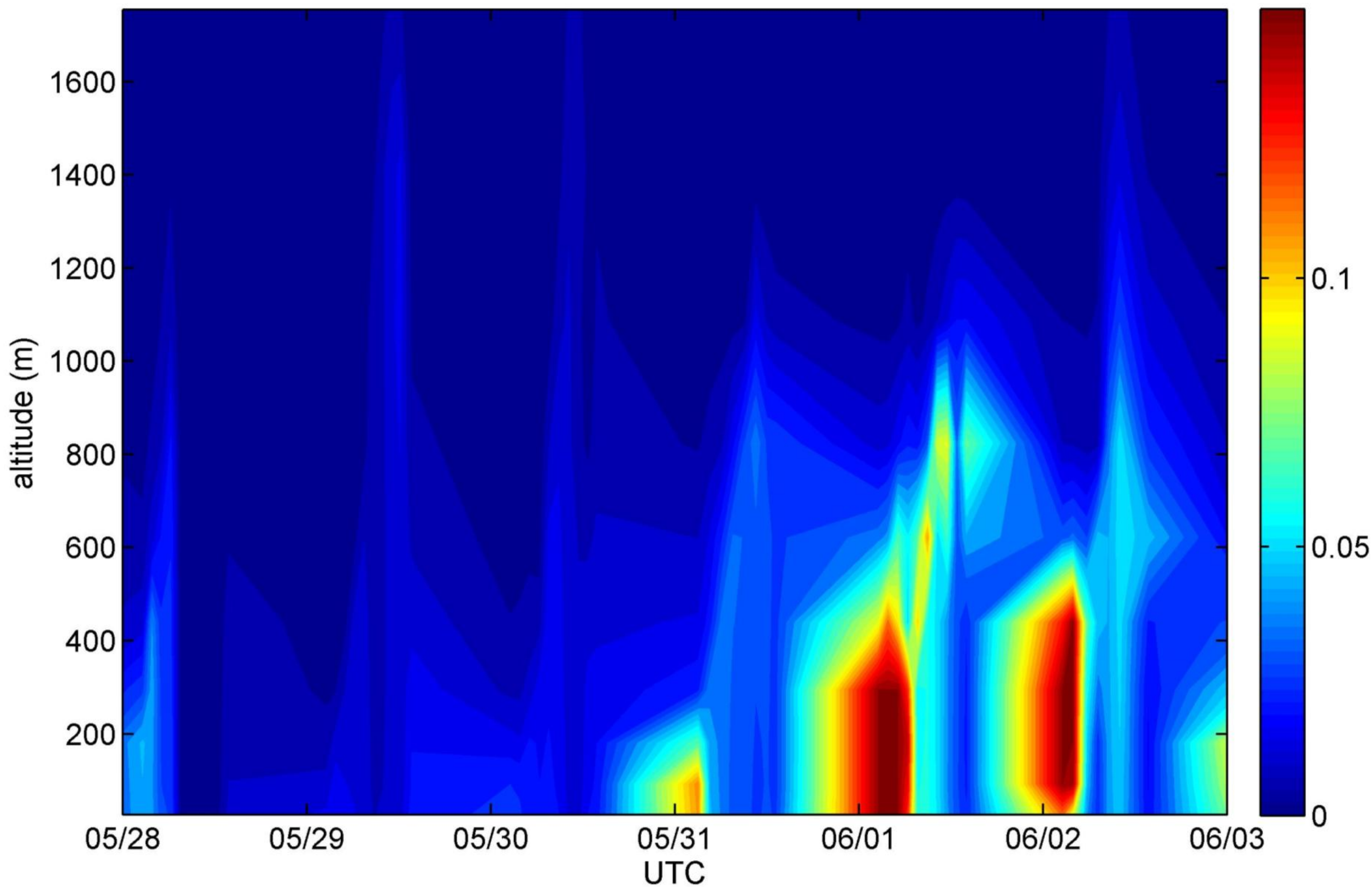

Comparison modeled and observed O_4

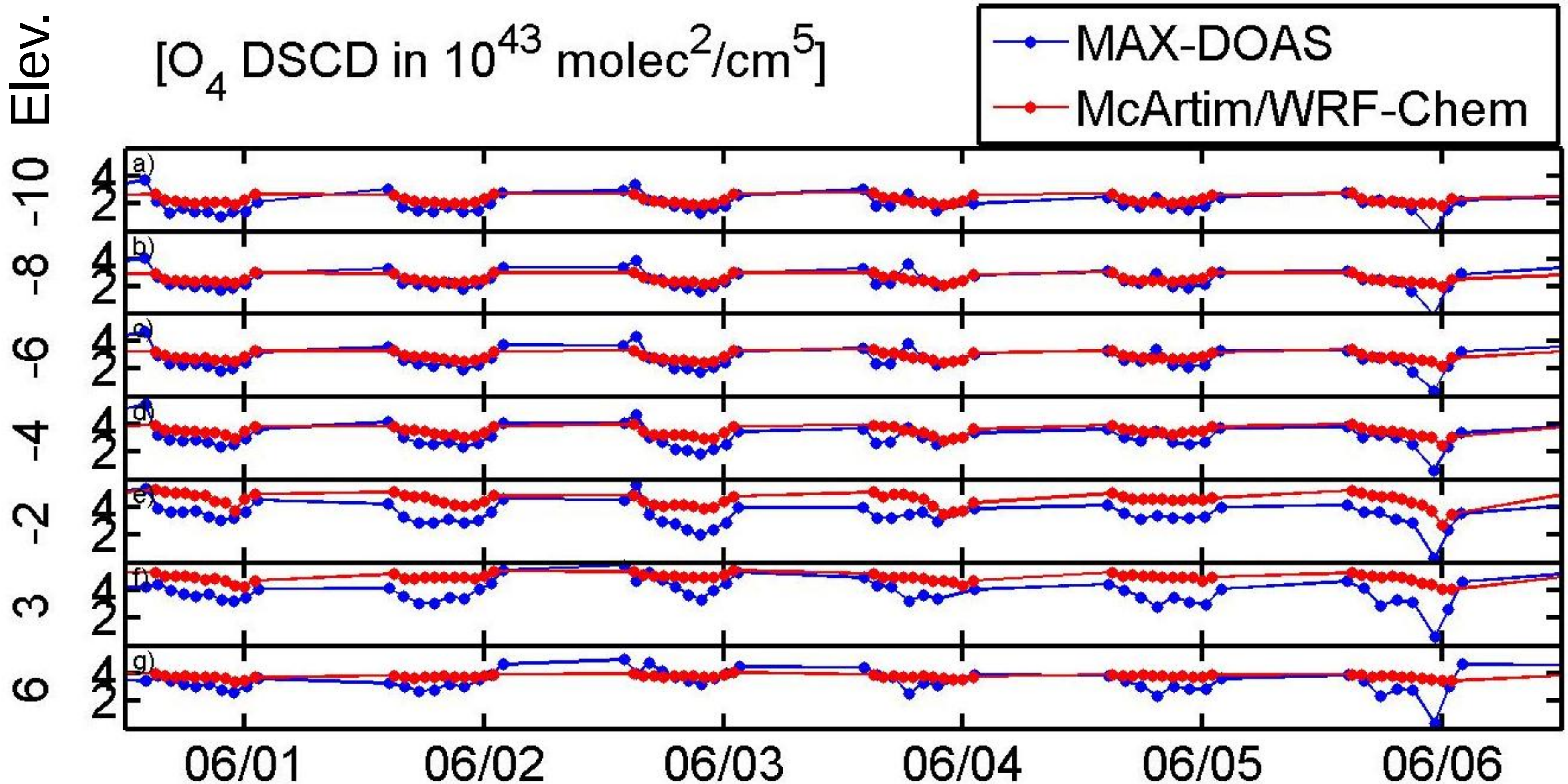

- Surprising good agreement for downward viewing angles
- Agreement in upper angles less good due to poor description of background aerosol.

Comparison modeled and observed NO_2

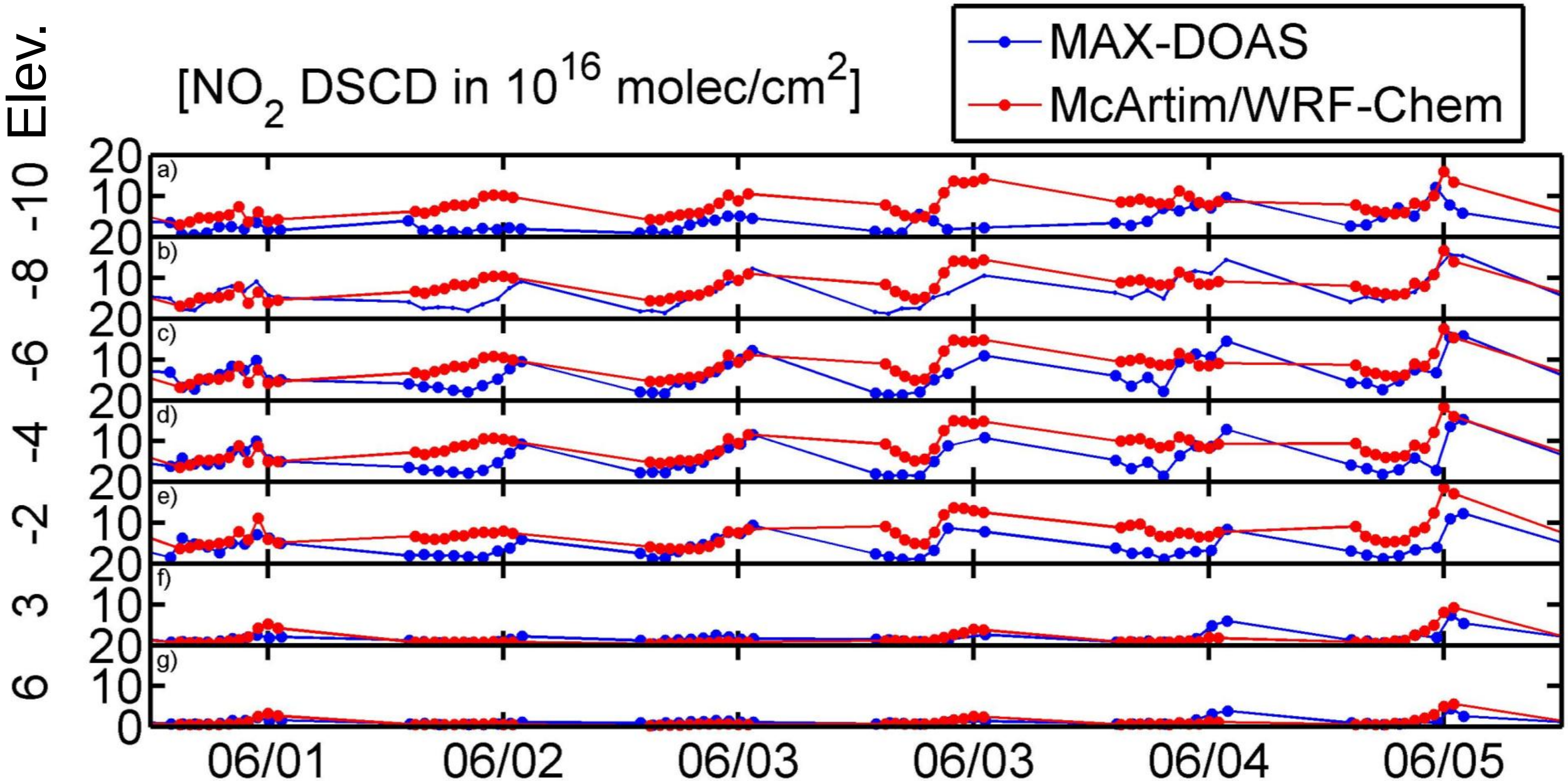

- Most NO_2 in boundary layer
- Model NO_2 higher than observations $\rightarrow$ emissions too high

$HCHO/NO_2$ as a measure of ozone sensitivity

- $HCHO/NO_2$ can be used to determine ozone sensitivity to NOx and VOCs [Martin et al., 2004 and Duncan et al., 2010]
- Duncan et al suggests HCHO/NO <1 in VOC-limited regimes and >2 in NO_x-limited regime.
- Highly constrained field observations during CalNex suggest the turn-over point for Los Angeles is $HCHO/NO_2$ ~ 0.55

As the vertical distribution of HCHO and NO_2 is similar UV observations can be use to determine this ratio without RT calculations

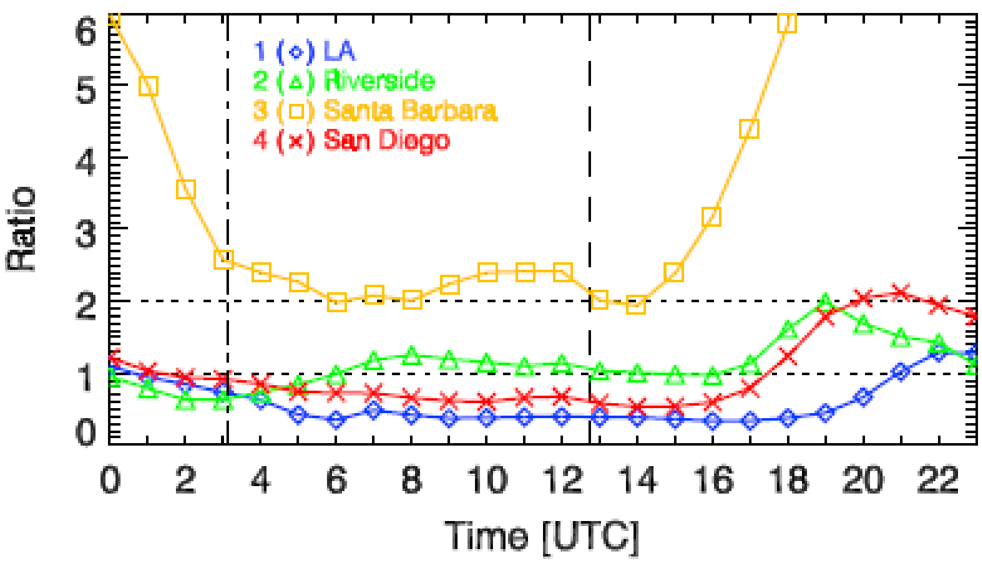

(Figure from Duncan et al., 2010)

MAX-DOAS $HCHO/NO_2$ ratio for CalNex LA

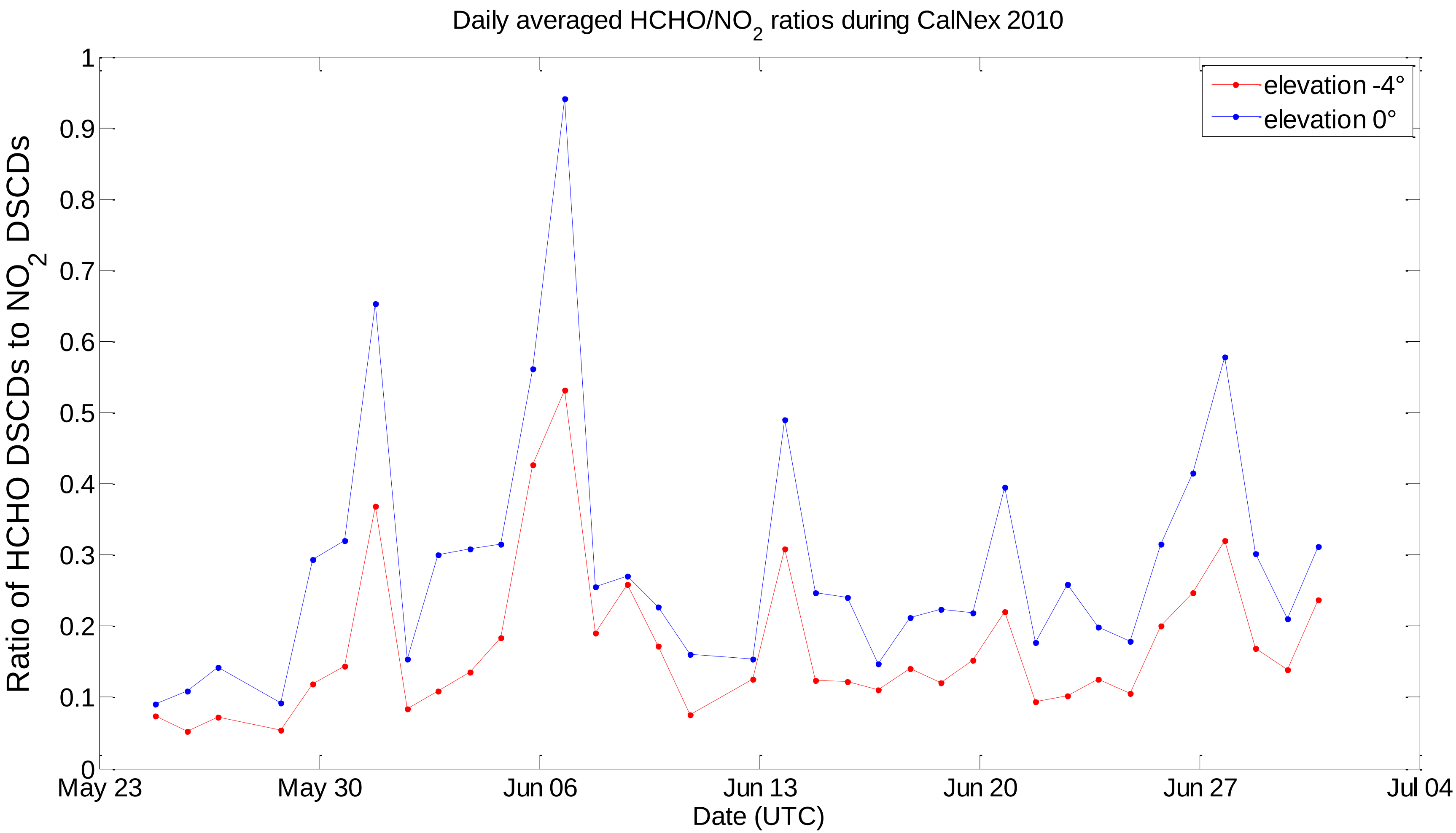

Clear Difference between Weekday and Weekend

MAX-DOAS HCHO/NO_2 ratio for two years

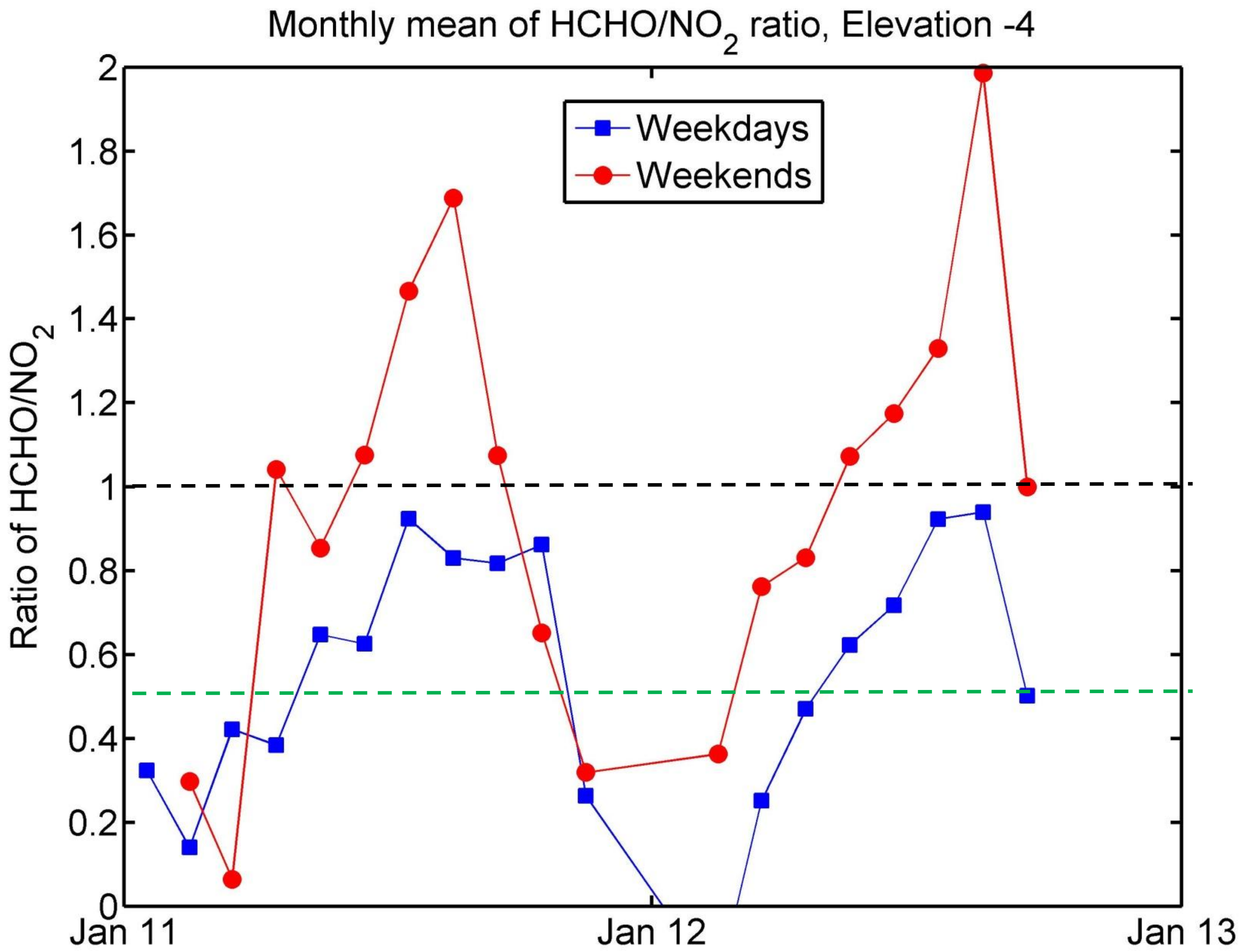

Retrieved in same wavelength range → no RT effects
Values between noon and 3pm local time

Weekend Effect

"Weekend effect" has been previously reported, where O_3 and NO_x levels reflect differences in driving patterns between weekdays and weekends

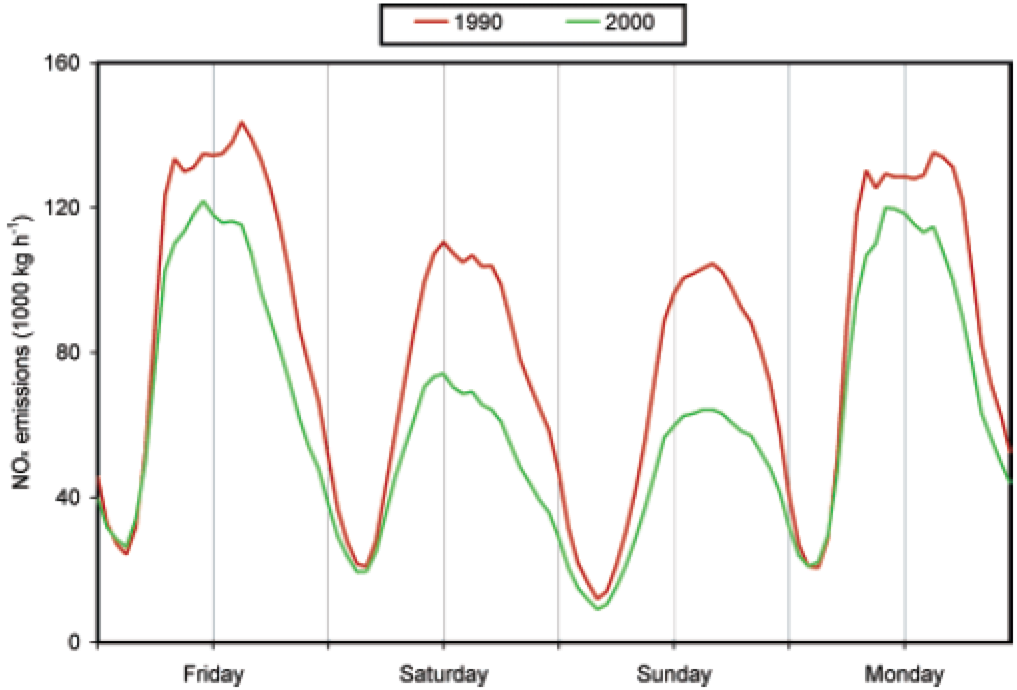

FIGURE 3. Change in statewide NO_x emissions from California on-road vehicles between 1990 (upper trace) and 2000 (lower trace). Values shown are the sum of gasoline and diesel engine emissions.

(Figure from Harley et al., 2005)

Annual Hourly Average NO_2 DSCD's

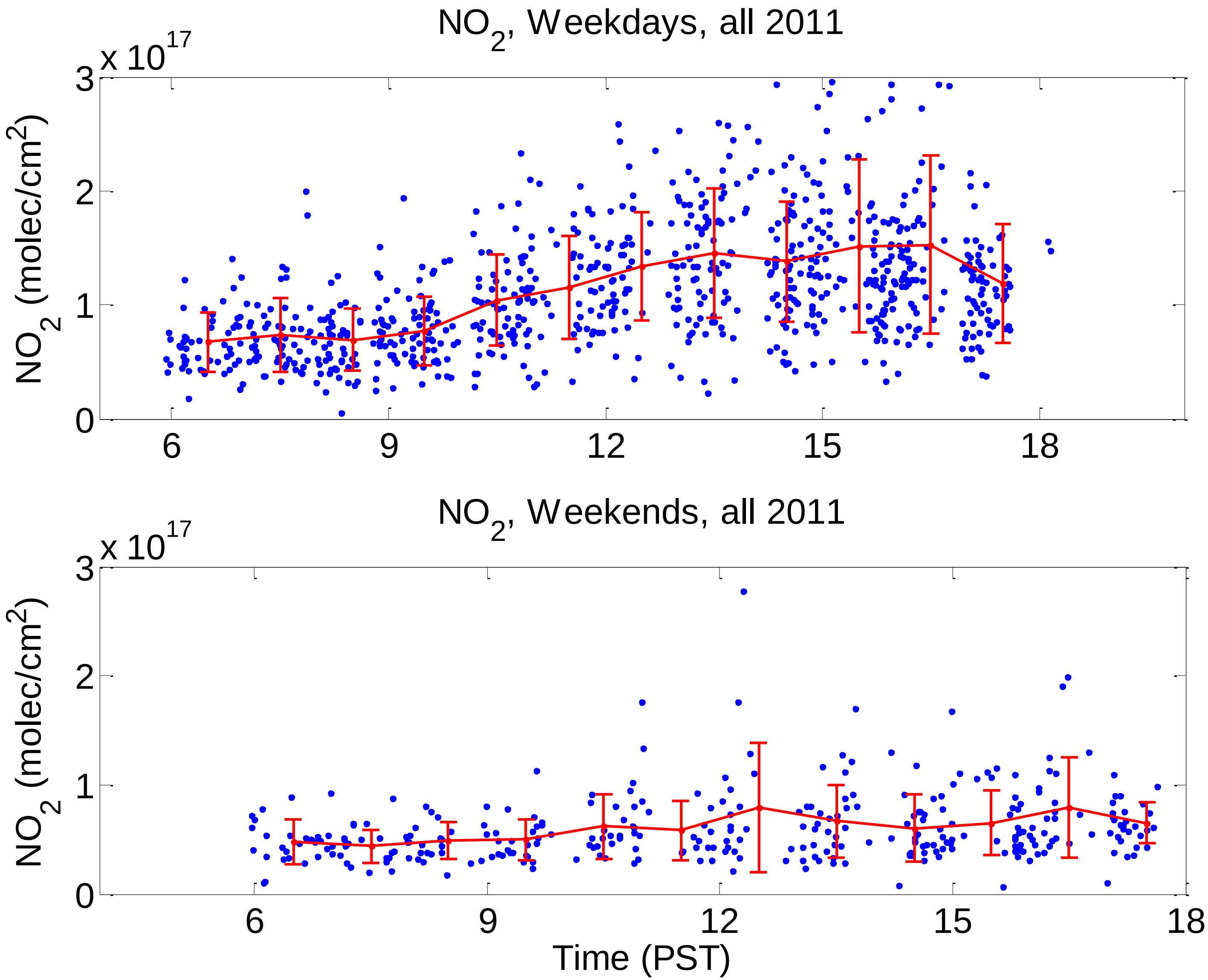

Lower NO_x on Weekends

Annual Hourly Average HCHO DSCD's

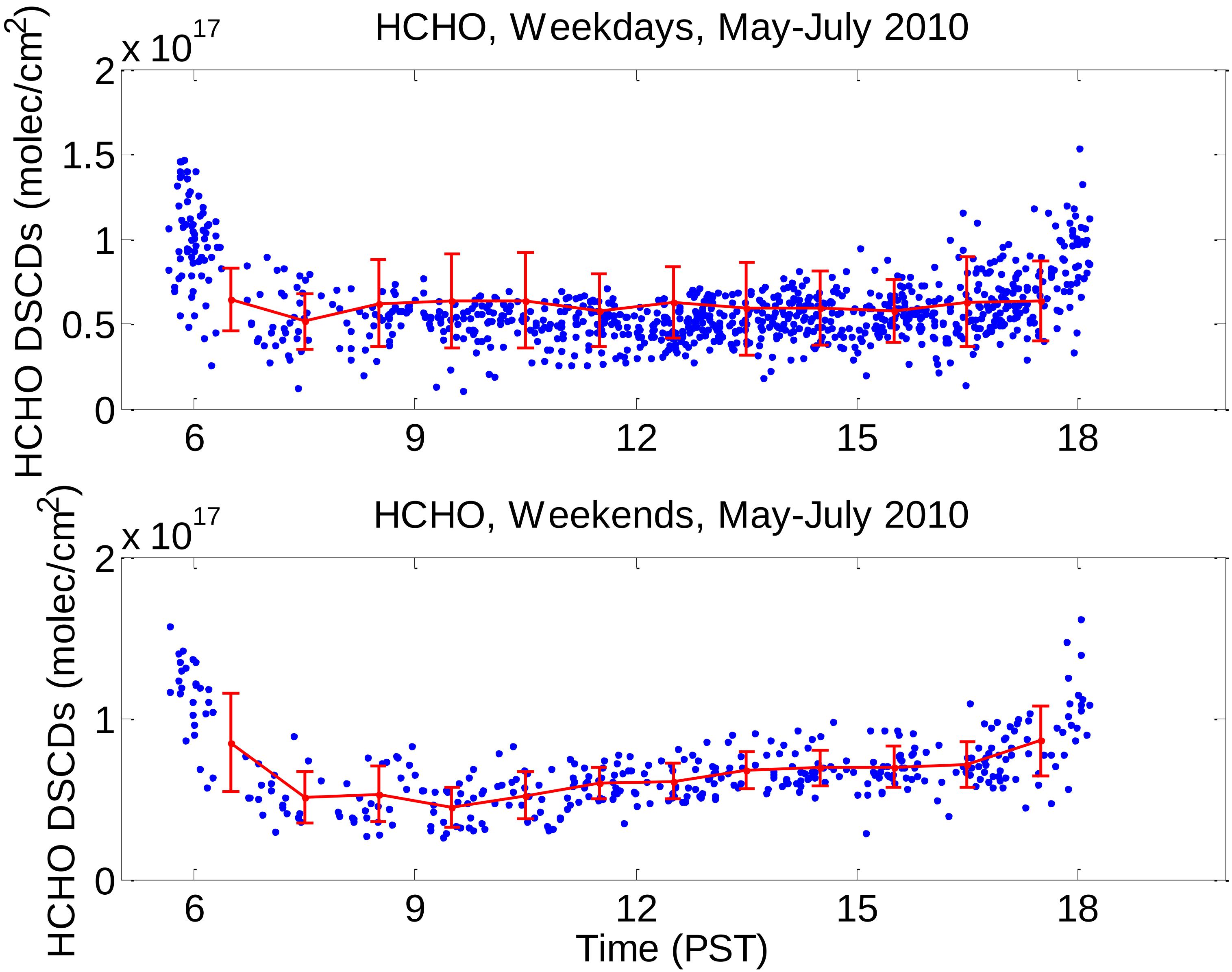

NO difference between Weekend and Weekday

Conclusions and Outlook

- Mountain-top remote sensing combined show great potential for monitoring of pollutants (and greenhouse gases).
- Direct comparison of the modeled with observed NO_2 looks promising.
- Longterm data gives insight into the NO_x/VOC sensitivity of ozone formation, the weekend effect, and longterm changes in NO_X and HCHO.
- Potential for satellite validation remains to be explored.
- Mountain sites can be a good test location of airborne or spaceborne instruments.

Acknowledgements

NASA Jet Propulsion Laboratory
for the use of CLARS

NOAA
CARB
for funding